JACS
JOURNAL OF THE AMERICAN CHEMICAL SOCIETY
pubs.acs.org/JACS
Article

Solvent Polarity under Vibrational Strong Coupling

Maciej Piejko, Bianca Patrahau, Kripa Joseph, Cyprien Muller, Eloïse Devaux, Thomas W. Ebbesen,* and Joseph Moran*

Cite This: https://doi.org/10.1021/jacs.3c02260
Read Online
ACCESS | Metrics & More | Article Recommendations | Supporting Information

ABSTRACT: Vibrational strong coupling (VSC) occurs when molecular vibrations hybridize with the modes of an optical cavity, an interaction mediated by vacuum fluctuations. VSC has been shown to influence the rates and selectivity of chemical reactions. However, a clear understanding of the mechanism at play remains elusive. Here, we show that VSC affects the polarity of solvents, which is a parameter well-known to influence reactivity. The strong solvatochromic response of Reichardt's dye (RD) was used to quantify the polarity of a series of alcohol solvents at visible wavelengths. We observed that, by simultaneously coupling the OH and CH vibrational bands of the alcohols, the absorption maximum of Reichardt's dye redshifted by up to ~15.1 nm, corresponding to an energy change of 5.1 kJ·mol^{-1}. With aliphatic alcohols, the magnitude of the absorption change of RD was observed to be related to the length of the alkyl chain and molecular surface area, indicating that dispersion forces are impacted by strong coupling. Therefore, we propose that dispersion interactions, which themselves originate from vacuum fluctuations, are impacted under strong coupling and are therefore critical to understanding how VSC influences chemistry.

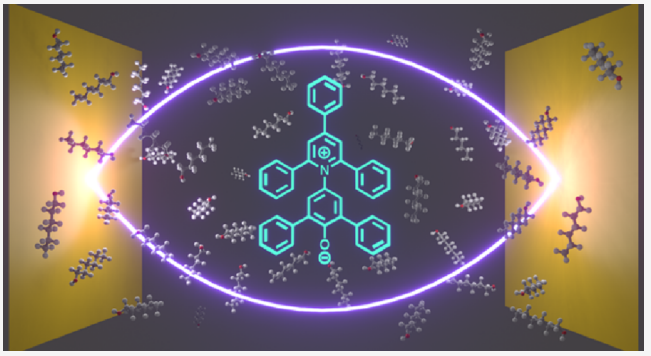

INTRODUCTION

Quantum fluctuations have measurable consequences. They belong to the domain of physics but can also impact chemical properties. Phenomena such as spontaneous emission,[1,2] the Casimir−Polder force,[3,4] Lamb shift,[3,5] or even London dispersion forces[1,4] all originate from the transient and omnipresent variations of the electromagnetic (EM) field in space. EM fluctuations are also key to understanding fundamental processes such as water autoprotolysis[6] or the surface-enhanced Raman effect.[7] Furthermore, they can be harnessed to directly modify chemical properties.[8,9]

Upon placing a molecule inside an optical cavity that is resonant with a selected vibrational mode, hybrid light-matter states are formed if energy is exchanged between the two faster than it dissipates. Under these conditions, a system is said to enter the vibrational strong coupling (VSC) regime,[8,10,11] which leads to the formation of two vibro-polaritonic bands (P+ and P−) and dark states (DSs) as shown in Figure 1A. This exotic interaction is mediated by EM fluctuations and therefore occurs even in the dark.[9,12] Over the past decade, it has been shown that VSC modifies a variety of chemical properties, such as reaction kinetics,[13−19] chemo-[14] and stereoselectivity,[18] ionic conductivity,[20] the rate of vibrational energy transfer,[21−26] selective crystallization,[27] or self-assembly.[28,29] The detailed mechanism at work is, however, still elusive, and more experimental results and theoretical analysis are needed.

Coupling-induced effects observed so far have been reported for (i) direct coupling of the reactant's vibrations,[13−15,18,19] (ii) cooperative coupling where a solvent vibration co-resonant with a vibrational band of the reactant is coupled,[17,30,31] or (iii) coupling of the solvent alone.[15] To understand case ii, it should be recalled that the rate of energy exchange between the cavity and the molecules needs to be faster than its dissipation. To achieve VSC, the energy splitting between the P+ and P− states, known as the Rabi splitting, must therefore be larger than the full width at half maximum (FWHM) of the vibrational band and the cavity mode. Since the Rabi splitting depends on the square root of the concentration ($\sqrt{C}$) of molecules coupled to the cavity mode,[8,9,32] VSC can be reached (i) by increasing the concentration of the solute or (ii) indirectly by coupling the solute via the solvent.

So far, the mechanism of VSC was mostly discussed in the context of the properties of the solute(s). Cases ii and iii raise the question of the importance and role of the solvent in the observed effects of VSC. Nevertheless, there has been no

Received: March 2, 2023

https://doi.org/10.1021/jacs.3c02260
J. Am. Chem. Soc. XXXX, XXX, XXX−XXX

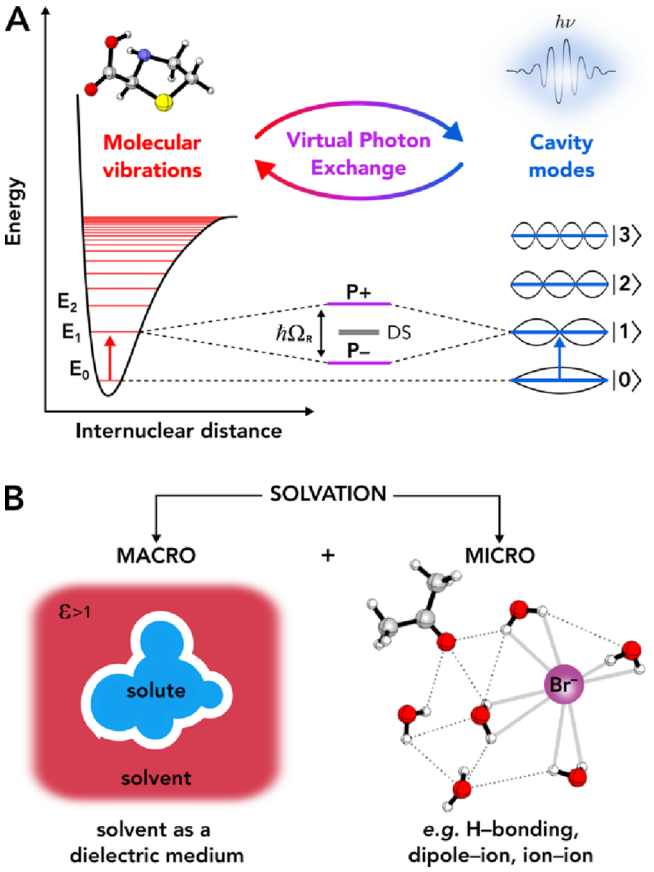

Figure 1. Solvent polarity under vibrational strong coupling. (A) Schematic diagram of the formation of the upper (P+) and lower (P−) vibro-polariton and degenerate dark states (DSs) from resonant vibrational and optical transitions. (B) Solvation can be seen in terms of a macroscopic effective medium and/or as a consequence of microscopic interactions between the solute and the solvent molecules.[36,37]

systematic study of the consequences of VSC on solvent properties such as its polarity.

Both the solvent's macroscopic bulk properties and its microscopic intermolecular interactions affect solvation (Figure 1B). In this view, macrosolvation would be impacted if strong coupling affects the solvent's relative permittivity and/or polarizability.[33,34] It has been shown recently that this is the case when coupling the OH stretching vibrations of water.[20] In a microscopic perspective of solvation (microsolvation), local interactions such as hydrogen bonding or dispersion interactions can also potentially be modified under strong coupling. Accordingly, solvation-sensitive systems, such as self-assembly,[28,29] enzyme-catalyzed reactions,[16,17] and proton transfers,[20,35] have been shown or predicted to be impacted by VSC.

Inspired by recent reports on the effect of solvent coupling,[15,20,28,29] we set out to study solvent properties under VSC by using Reichardt's dye (RD), which is a solvent polarity probe.[36,37] RD exhibits an exceptionally strong negative solvatochromism, which allows one to detect subtle differences in polarity and solvent properties.[38−40] To measure the change in polarity, we used the $E_T(30)$ polarity parameter, which is defined as the molar electronic transition energy of RD[36]

$$E_T(30) = \frac{hcN_A}{\lambda_{max}}$$

where h, c, and N_A are Planck's constant, the speed of light, and Avogadro's constant, respectively. λ_{max} is the absorption maximum of the polarity-sensitive intramolecular charge transfer (CT) band. λ_{max} is known to shift across the whole visible spectrum from the near-IR region for nonpolar solvents to the UV region for polar solvents such as water (Figure 2).

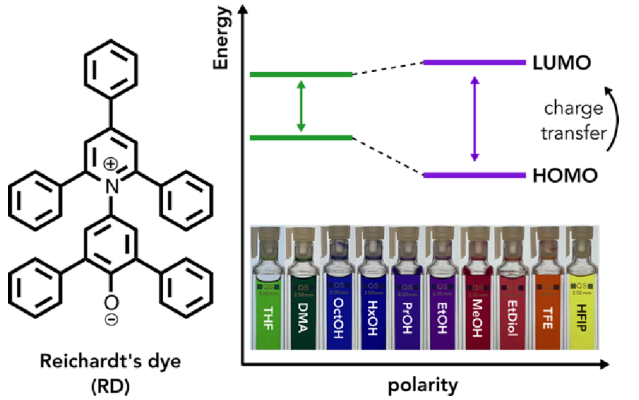

Figure 2. Chemical structure of Reichardt's dye (left panel). The degree of ground-state stabilization in various solvents due to the high dipole moment of the molecule changes the HOMO−LUMO gap significantly (right panel). The gap increases with increasing solvent polarity (negative solvatochromism). The CT band spans the whole visible spectrum due to its sensitivity. Pictures of RD solutions in solvents of increasing polarity from left to right are shown. Abbreviations used: THF - tetrahydrofuran, DMA - dimethylacetamide, OctOH - 1-octanol, HxOH - 1-hexanol, PrOH - 1-propanol, EtOH - ethanol, MeOH - methanol, EtDiol - 1,2-ethanediol, TFE - trifluoroethanol, and HFIP - hexafluoroisopropanol.

As thoroughly studied by Sander et al., the position of this CT band is mostly affected by bulk properties, whereas local molecular interactions only mildly affect its spectral response.[38] Nonetheless, they show that, when the dye interacts with hydrogen-bond donors, it is much more sensitive to bulk polarity changes. These features of RD, along with its good solubility in a variety of organic solvents and its high absorption coefficient, make it a suitable choice for studying polarity under VSC.

RESULTS AND DISCUSSION

To elucidate the effects of VSC on polarity, we compared the absorption spectra of 30 mM solutions of RD in a variety of alcohols, which are vibrationally coupled to one or more cavity modes in the IR region. We used Fabry-Perot cavities, which consist of two parallel mirrors confining the EM field. The dye itself is not concentrated enough to achieve strong coupling with the cavity field. We performed three distinct types of experiments: on-resonance cavity experiments, off-resonance cavity experiments, and cell measurements. In an on-resonance cavity experiment, one or more optical modes are resonant with a vibrational band of the solvent at normal incidence to the cavity. It has been shown in numerous experiments that ground-state properties are only modified by VSC under these conditions.[8,9] In an off-resonance experiment, the cavity is detuned to avoid any coupling, serving as the first type of control experiment. Figure S2 shows a typical microfluidic

https://doi.org/10.1021/jacs.3c02260
J. Am. Chem. Soc. XXXX, XXX, XXX−XXX

setup used for such cavity measurements. A cell experiment is performed in a similar setup lacking the reflective gold layer. Since it is not an optical cavity, VSC cannot occur, and therefore it serves as the second type of control experiment. The results of these three types of experiments were then compared to assess the effect of VSC. Unless stated otherwise, 25 μm-thick Mylar spacers were used in both cavity and cell experiments. For more details about cavity preparation and measurements, see the corresponding section in the Supporting Information. The core experimental workflow is as follows (Figure 3). First, a neat solvent is injected into an on-resonance cavity. The coupling is monitored by recording an infrared spectrum. Subsequently, the visible absorption spectrum of the same cavity is acquired. Then, the cavity is emptied by flushing with nitrogen and a solution of RD in the same solvent is injected. An IR spectrum is recorded again to confirm that the coupling remains unchanged, and lastly, an absorption spectrum is recorded. The spectrum of neat solvent is subtracted from the spectrum of the dye, and the absorption maximum of the CT band is determined. In some cases, additional smoothing of the absorption spectrum using the moving average method is required due to Fabry–Perot interference inherent to the cavity (see Figure S6). The same procedure is repeated in a microfluidic cell with an identical path length but without the reflective gold layer. All experiments were performed at least three times, and the standard error calculation is explained in the Supporting Information.

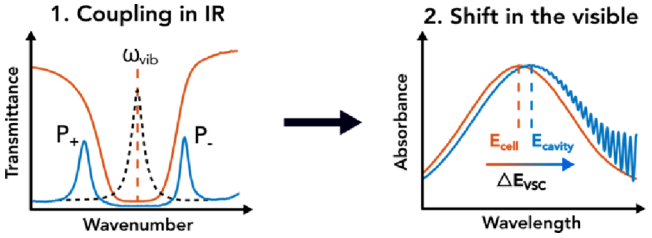

Figure 3. Experimental workflow. The coupling is monitored by FTIR spectroscopy. After achieving the desired coupling state (on/off-resonance), an absorption spectrum in the visible region is recorded and the position of the maximum of the CT band is determined to calculate the $E_T(30)$ polarity parameter and the cavity-induced shift (ΔE_{VSC}).

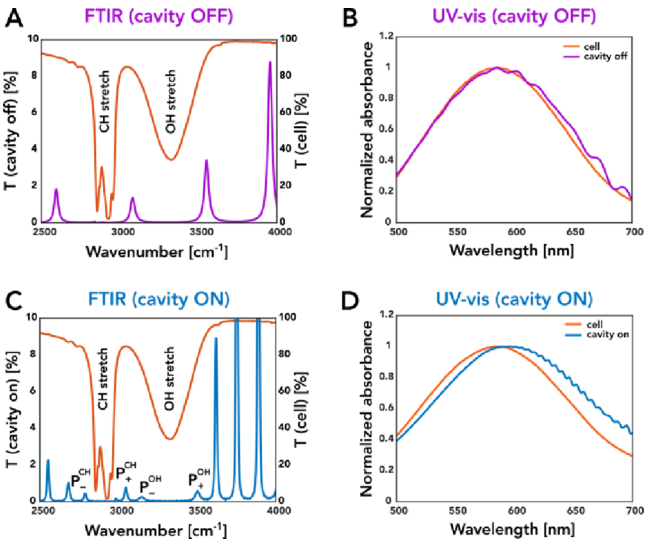

Figure 4. VSC-induced shift. (A, B) Off-resonance FTIR and UV–vis spectra, respectively, of 1-nonanol in a cell (orange) and cavity (violet). (C, D) On-resonance FTIR and UV–vis spectra, respectively, of 1-nonanol in a cell (orange) and cavity (blue). The appearance of inhomogeneous shifting is due to the smoothing applied to the cavity spectrum to reduce the Fabry–Perot interference inherent to optical cavities (for details, see the Supporting Information).

The observed changes in the transition wavelength of RD $\Delta\lambda_{VSC}$ is given by the spectral shift at the absorption maxima

$$\Delta\lambda_{VSC} = \lambda_{max}^{cavity-on} - \lambda_{max}^{cell}$$

from which the difference ΔE_{VSC} between the transition energy of the on-resonance cavities ($E_{cavity\text{-}on}$) and cell experiments (E_{cell}) is obtained:

$$\Delta E_{VSC} = E_{cavity-on} - E_{cell}$$

First, we studied solutions of RD in 1-nonanol by coupling the OH and CH stretching bands simultaneously, which was unavoidable due to their proximity and width. The Rabi splitting of the bands were 355 and 195 cm^{-1} and were larger than the FWHM of the cavity mode and the vibrational bands (19 and 300 cm^{-1}), confirming that the solvent was under VSC. Interestingly, we observed a 12.9 ± 1.0 nm redshift of the CT band in the visible region (Figure 4). Off-resonance cavity experiments were performed to confirm that the effect is due to strong coupling. The result was identical to that of cell experiments ($\lambda_{max}^{cavity\ -\ off}$ = 584.0 ± 0.6 nm and λ_{max}^{cell} = 584.4 ± 0.2 nm), confirming that the effect depends on cavity tuning and resonance.

Encouraged by this result, we then studied a series of linear alcohols from methanol to decanol under VSC. As can be seen in Figure 5 (blue points), a remarkable trend is observed. The RD solvatochromic change induced by VSC increases with the length of the hydrocarbon moiety of the alcohol. The sign of $\Delta\lambda_{VSC}$ was always negative (redshift), which indicates that the alcohols become less polar.

What is the reason for this behavior? Besides its known solvatochromism, RD was reported to show thermochromism, piezochromism, and halochromism.[40] We measured the temperature dependence of λ_{max} and concluded that the thermochromic shift is only relevant above 25 °C (Figure S11), which is in agreement with other studies of RD and its derivatives.[41,42] For this reason, the working temperature was always kept at 22 ± 1 °C. Since all measurements were performed under atmospheric pressure and without the addition of salts, piezochromism and halochromism are irrelevant in our experiments. RD is also known to form aggregates,[43] which potentially could affect the absorption spectrum. However, the CT band does not shift in a wide concentration range between 4·10^{-5} and 10^{-1} M, which includes solutions containing the dye in both its monomeric and aggregated state (Figure S11). The spectrum of RD is therefore unaffected by aggregation. We also considered the possibility that cooperative VSC between solvent and RD might produce the observed shifts. However, we found no correlation between the observed spectral shift and the degree of overlap of the solvent and RD bands, which are not visible in solution due to the low intensity (see Figure S15).

To obtain further insight into the observed trend with the alcohol chain length, we first explored whether the coupling strength (Rabi splitting) influences the magnitude of the

https://doi.org/10.1021/jacs.3c02260
J. Am. Chem. Soc. XXXX, XXX, XXX−XXX

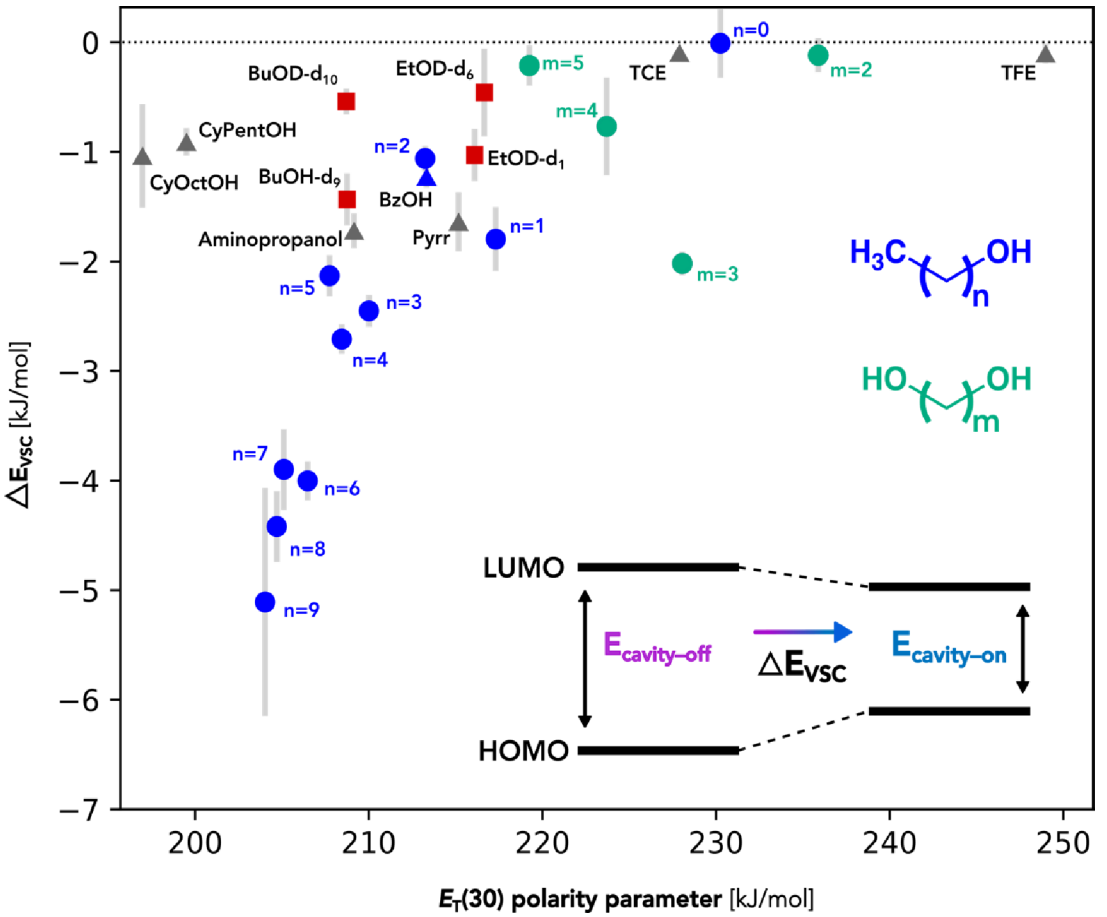

Figure 5. Dependence of the VSC-induced shift on the $E_T(30)$ polarity parameter. In most studied cases, by vibrationally coupling the solvent, the CT band of RD redshifts, which corresponds to a decrease of effective polarity. Color and shape code: linear alcohols - blue circles, terminal diols - green circles, deuterated alcohols - red squares, and other alcohols - gray triangles. The depicted relative energy difference of HOMO and LUMO levels in on- and off-resonance cavity experiments is purely indicative. Abbreviations used: TCE - 2,2,2-trichloroethanol, TFE - 2,2,2-trifloroethanol, BzOH - benzyl alcohol, Pyrr - pyrrole, CyPentOH - cyclopentanol, and CyOctOH - cyclooctanol.

f6 change. As can be seen in Figure 6, upon increasing the hexanol concentration in a binary mixture of hexanol and deuterated dichloromethane, an abrupt solvatochromic change is observed at the onset of strong coupling. Otherwise, the spectral shift is independent of the Rabi splitting within experimental error. This sudden change in polarity is reminiscent of a phase transition, which has also been reported for CT complexes under VSC.[44]

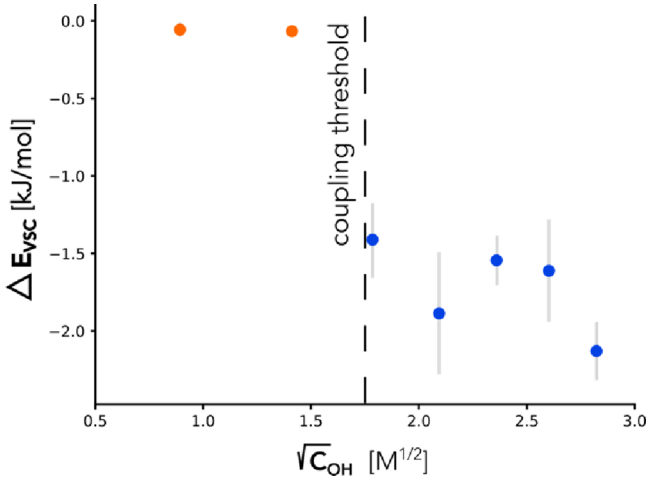

Figure 6. Dependence of ΔE_{VSC} on the coupling strength, which is proportional to $\sqrt{C}$. Upon reaching the strong coupling threshold, the CT band of RD abruptly redshifts.

It is also interesting to evaluate the effect and contribution of coupling of the hydrogen-bond donating moiety. However, as mentioned before, in our conditions, it was impossible to selectively study the effect of OH coupling due to the proximity of the CH band. Nevertheless, it is possible to couple the CH vibrations alone, but no effect was observed (see the Supporting Information), pointing to the importance of coupling the OH band. This was confirmed by studying pyrrole as its NH stretching band is thinner and well-isolated and it can be coupled selectively. Upon coupling this band, the RD signal shifts by 4.3 ± 0.7 nm ($\Delta E_{VSC} = -1.6 \pm$ kJ·mol^{-1}). This effect vanishes after detuning the cavity (off-resonance). It suggests that coupling the band of the hydrogen-bonded functional group is essential to induce a significant shift. This is consistent with the fact that the response of RD is enhanced by hydrogen bonding.[38]

Interestingly, in contrast to the clear trend observed for linear alcohols, none were observed for related classes of compounds. For instance, a series of terminal diols were compared by changing the length of the aliphatic chain. No shift was observed for 1,2-ethanediol, yet 1,3-propanediol gave

https://doi.org/10.1021/jacs.3c02260
J. Am. Chem. Soc. XXXX, XXX, XXX−XXX

$\Delta\lambda_{VSC} = 4.7 \pm 0.3$ nm. However, the shift decreased and nearly vanished with further increases in the chain length (green points in Figure 5). A rationale for this observation is not clear. Perhaps it stems from the interplay of the two opposing terminal dipoles and the length and therefore the rigidity of the molecule. Next, we tested a series of alcohols of different structures and chemical properties and found no correlation except that the polarity was always reduced under VSC (gray triangles in Figure 5).

We also compared the effect of OH and CH deuteration on the observed shift under strong coupling (red squares on Figure 5). Deuteration not only lowers the vibrational energy but also introduces subtle modifications to the molecular geometry and polarity.[45−49]

Due to the lower polarizability of the deuterated compounds, dispersion forces between deuterated molecules are weaker. This can be understood by considering the well-known formula for the dispersion energy between two atoms (A and B) derived by London and Eisenschitz.[50] This shows that this interaction rapidly decreases with interatomic separation R and depends also on static polarizabilities of the interacting partners (α_A^0 and α_B^0)

$$E_{AB}^{disp} = -\frac{C}{R^6}$$

$$C = \frac{3}{2}\frac{I_A I_B}{I_A + I_B}\alpha_A^0 \alpha_B^0$$

where I_A and I_B are the atomic ionization potentials. In the case of ethanol, the gradual substitution of protons for deuterium atoms (EtOH → EtOD-d_1 → EtOD-d_6) indeed decreases the RD shift under VSC. Similarly, for perprotiated butanol (BuOH), a significant shift of -2.5 ± 0.1 kJ·mol^{-1} is observed but almost vanishes in perdeuterated BuOD-d_{10} and BuOH-d_9 (-0.2 ± 0.1 and -0.5 ± 0.2 kJ·mol^{-1}, respectively).

Dispersion forces are also known to depend on the molecular shape. This can be seen when comparing boiling points of molecules in which the only interaction present is dispersion—hydrocarbons. At atmospheric pressure, linear *n*-pentane boils at 36.1 °C, branched isopentane boils at 27.8 °C, and the near-spherical neopentane boils at

9.5 °C. Branching decreases the surface area of the molecule and, with it, the magnitude of dispersion forces. For this reason, we compared ΔE_{VSC} in C5 alcohols with different connectivities (Figure 7). We compared the effect with the solvent accessible surface area (SASA) as this is the area that is accessible for intermolecular interactions.[51,52] Linear 1-pentanol has the highest surface area. The area decreases with branching (2-pentanol and isopentanol) and is the lowest for the cyclopentanol. ΔE_{VSC} is clearly proportional to the surface area, showing that dispersion interactions are modified under VSC.

Thus, the influence of deuteration, alkyl chain length, and molecular surface area on ΔE_{VSC} indicate that the impact of VSC on solvent polarity arises from the modification of London dispersion forces between the solvent and the dye and/or the solvent molecules. Indeed, dispersion forces originate from quantum fluctuations[3,4] and therefore are most likely altered by strong coupling since it enhances interactions with the vacuum field at resonant frequencies. This agrees with several theoretical reports, which suggest that dispersion is modified under strong coupling.[3,53] However, it is still not understood why this leads to a decrease in the polarity of nearly all alcohols studied (Figure 5).

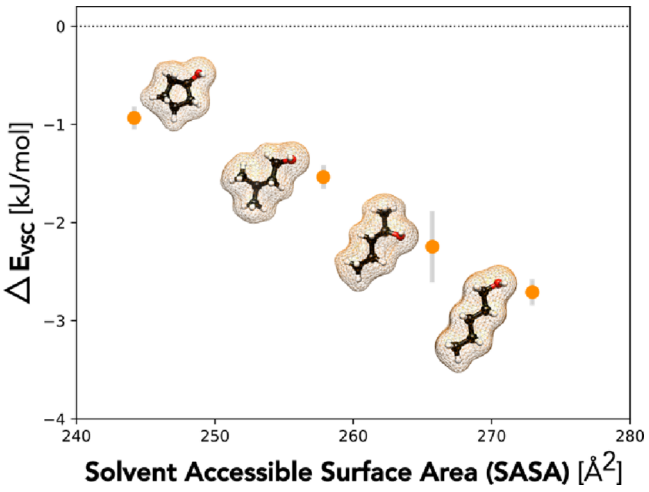

Figure 7. Dependence of the VSC-induced shift on the solvent accessible surface area (SASA) for C5 alcohols. ΔE_{VSC} increases proportionally to the surface area in the following order: cyclopentanol, isopentanol, 2-pentanol, and 1-pentanol.

While the shift in the response of RD under VSC mostly reflects changes in bulk properties, it is possible that specific solvent−solvent and/or solvent−dye interactions are perturbed. The dynamics and structure of the solvent could also be modified by VSC without being detected by RD. For this reason, we also plotted the shift against other parameters, which indirectly reflect intermolecular interactions, such as the surface tension and viscosity. As can be seen in Figure S81, a linear correlation is observed between the changes induced in the series of aliphatic alcohols and the surface tension of these compounds. This supports the role of dispersion interactions under strong coupling since it is known that surface tension is a good measure of dispersion forces in hydrocarbons.[54] It should be recalled that these experiments involve coupling of many solvent molecules, resulting in collective delocalized states. This likely explains the phase transition-like behavior observed in Figure 6. In turn, this suggests that the collective delocalized states and possibly their coherence might play a role in modifying the properties of the solvent such as polarity.

Notably, the described results can be compared with other studies in which dispersion forces might play an important role. For instance, the effect of deuteration recalls the case of VSC-induced acceleration of enzymatic ester hydrolysis upon coupling the OH stretching band of water.[17] In that study, the gradual introduction of D_2O instead of H_2O decreased the extent of acceleration. Another comparison can be made with the case of urethane formation studied under VSC.[15] When coupling the C−H stretching bands of the solvent (tetrahydrofuran), the reaction rate decreased, which also could be caused by changes in the solvation of the reactants. Self-assembly[28,29] is also affected by the VSC of the solvent as well as the ionic conductivity and permittivity of water.[20]

In this work, we have shown that VSC changes solvent polarity, which has clear implications for chemical reactivity under VSC. One might ask whether this effect is responsible for the altered reactivity observed in previously reported VSC studies and especially in reported cases of reactions run in alcohols as solvents. For example, the seminal study on changing the rate of silyl deprotection under VSC was

https://doi.org/10.1021/jacs.3c02260
J. Am. Chem. Soc. XXXX, XXX, XXX−XXX

conducted in methanol.[13] However, in the present study, no polarity change was observed in this solvent. In another study in which the selectivity of silyl deprotection of two different functional groups was modified under VSC,[14] a 1:1 binary mixture of MeOH/THF was used. To relate this to our study, we checked whether the polarity of such a solvent system could be impacted by VSC. Interestingly, upon coupling both the O−H (~3500 cm^{-1}) and C−O (~1050 cm^{-1}) stretches in a solution of RD, a decrease in polarity was observed (ΔE_{VSC} = −2.6 ± 0.1 $kJ \cdot mol^{-1}$). A decrease in polarity would be expected to increase the reactivity (nucleophilicity) of the fluoride anion,[55] which in turn should increase the rate of deprotection. Instead, the authors reported a rate decrease, which suggests that a solvent polarity change was not the main factor influencing reactivity in that specific case. This is consistent with a previous theoretical study, which indicated that other factors, such as a modified vibrational energy redistribution, govern the reactivity under strong coupling.[25] Therefore, our work highlights that a better understanding of the consequences of VSC on intra- and intermolecular interactions is necessary and evidences the key role of dispersion forces. Further studies regarding the role of dispersion forces in substrate molecules under VSC should bring important insight to the field of polaritonic chemistry.

CONCLUSIONS

We studied how VSC impacts the polarity upon coupling alcoholic solvents as measured by the solvatochromic response of Reichardt's dye. In most studied alcohols, the absorption spectrum of the dye exhibits a redshift in the visible range, which corresponds to an effective decrease in polarity. Although no shift was observed for short-chained systems, such as methanol or ethylene glycol, a large shift of up to ~15.1 nm is observed for longer aliphatic alcohols, indicating a significant change in solvent polarity. The observed trend in the spectral shift indicates that dispersion interactions are the key factor guiding the behavior of the system. Nevertheless, other VSC-induced microscopic modifications might also be occurring that are not detected by RD. Changes in solvent properties need to be considered in studies of modified reactivity and other physical chemistry studies under VSC.

ASSOCIATED CONTENT

Supporting Information

The Supporting Information is available free of charge at https://pubs.acs.org/doi/10.1021/jacs.3c02260.

Details of experimental procedures, FTIR and UV−vis spectra, description of the data treatment, and correlations of other solvent-describing parameters (PDF)

AUTHOR INFORMATION

Corresponding Authors

Thomas W. Ebbesen − *University of Strasbourg, CNRS, ISIS and icFRC, 67000 Strasbourg, France;* orcid.org/0000-0002-3999-1636; Email: ebbesen@unistra.fr

Joseph Moran − *University of Strasbourg, CNRS, ISIS and icFRC, 67000 Strasbourg, France;* orcid.org/0000-0002-7851-6133; Email: moran@unistra.fr

Authors

Maciej Piejko − *University of Strasbourg, CNRS, ISIS and icFRC, 67000 Strasbourg, France;* orcid.org/0000-0002-2742-5688

Bianca Patrahau − *University of Strasbourg, CNRS, ISIS and icFRC, 67000 Strasbourg, France*

Kripa Joseph − *University of Strasbourg, CNRS, ISIS and icFRC, 67000 Strasbourg, France*

Cyprien Muller − *University of Strasbourg, CNRS, ISIS and icFRC, 67000 Strasbourg, France*

Eloïse Devaux − *University of Strasbourg, CNRS, ISIS and icFRC, 67000 Strasbourg, France*

Complete contact information is available at: https://pubs.acs.org/10.1021/jacs.3c02260

Funding

We acknowledge the support of the International Center for Frontier Research in Chemistry (icFRC, Strasbourg), Labex NIE projects (ANR-11-LABX-0058 NIE), and CSC (ANR-10-LABX- 0026 CSC) within the Investissement d'Avenir program ANR-10-IDEX-0002-02. M.P. thanks the CSC Graduate School funded by the French National Research Agency (no. CSC-IGS ANR-17-EURE-0016). T.W.E. and J.M. both acknowledge the support of the ERC (project nos. 788482 MOLUSC and 101018894 Metabolism Origins, respectively).

Notes

The authors declare no competing financial interest.

ACKNOWLEDGMENTS

The authors would like to thank Dr. Robert Mayer and Dr. Soh Kushida for useful advice and fruitful scientific discussions.

ABBREVIATIONS

EM electromagnetic
VSC vibrational strong coupling
RD Reichardt's dye
CT charge transfer

REFERENCES

(1) Milonni, P. W. Why spontaneous emission? *Am. J. Phys.* **1984**, *52*, 340−343.
(2) Haroche, S.; Kleppner, D. Cavity quantum electrodynamics. *Phys. Today* **1989**, *42*, 24−30.
(3) Buhmann, S. Y.; Welsch, D.-G. Dispersion forces in macroscopic quantum electrodynamics. *Prog. Quantum Electron.* **2007**, *31*, 51−130.
(4) Dzyaloshinskii, I. E.; Lifshitz, E. M.; Pitaevskii, L. P. The general theory of van der Waals forces. *Adv. Phys.* **1961**, *10*, 165−209.
(5) Welton, T. A. Some observable effects of the quantum-mechanical fluctuations of the electromagnetic field. *Phys. Rev.* **1948**, *74*, 1157.
(6) Turi, L.; Rodriguez, J.; Laria, D. Combined Effects from Solvation and Nuclear Quantum Fluctuations on Autoionization Mechanisms in Aqueous Clusters. *J. Phys. Chem. B* **2020**, *124*, 2198−2208.
(7) Langer, J.; Jimenez de Aberasturi, D.; Aizpurua, J.; Alvarez-Puebla, R. A.; Auguié, B.; Baumberg, J. J.; Bazan, G. C.; Bell, S. E. J.; Boisen, A.; Brolo, A. G.; Choo, J.; Cialla-May, D.; Deckert, V.; Fabris, L.; Faulds, K.; García de Abajo, F. J.; Goodacre, R.; Graham, D.; Haes, A. J.; Haynes, C. L.; Huck, C.; Itoh, T.; Käll, M.; Kneipp, J.; Kotov, N. A.; Kuang, H.; Le Ru, E. C.; Kwee Lee, H.; Li, J.-F.; Ling, X.-Y.; Maier, S. A.; Mayerhöfer, T.; Moskovits, M.; Murakoshi, K.; Nam, J.-M.; Nie, S.; Ozaki, Y.; Pastoriza-Santos, I.; Perez-Juste, J.; Popp, J.; Pucci, A.; Reich, S.; Ren, B.; Schatz, G. C.; Shegai, T.; Schlücker, S.;

Tay, L.-L.; Thomas, K. G.; Tian, Z.-Q.; Van Duyne, R. P.; Vo-Dinh, T.; Wang, Y.; Willets, K. A.; Xu, C.; Xu, H.; Xu, Y.; Yamamoto, Y. S.; Zhao, B.; Liz-Marzán, L. M. Present and future of surface-enhanced Raman scattering. *ACS Nano* **2019**, *14*, 28−117.

(8) Nagarajan, K.; Thomas, A.; Ebbesen, T. W. Chemistry under vibrational strong coupling. *J. Am. Chem. Soc.* **2021**, *143*, 16877−16889.

(9) Garcia-Vidal, F. J.; Ciuti, C.; Ebbesen, T. W. Manipulating matter by strong coupling to vacuum fields. *Science* **2021**, *373*, No. eabd0336.

(10) Galego, J.; Climent, C.; Garcia-Vidal, F. J.; Feist, J. Cavity Casimir-Polder forces and their effects in ground-state chemical reactivity. *Phys. Rev. X* **2019**, *9*, No. 021057.

(11) Shalabney, A.; George, J.; Hutchison, J. A.; Pupillo, G.; Genet, C.; Ebbesen, T. W. Coherent coupling of molecular resonators with a microcavity mode. *Nat. Commun.* **2015**, *6*, 1−6.

(12) Jaynes, E. T.; Cummings, F. W. Comparison of quantum and semiclassical radiation theories with application to the beam maser. *Proc. IEEE* **1963**, *51*, 89−109.

(13) Thomas, A.; George, J.; Shalabney, A.; Dryzhakov, M.; Varma, S. J.; Moran, J.; Chervy, T.; Zhong, X.; Devaux, E.; Genet, C.; Hutchison, J. A.; Ebbesen, T. W. Ground-state chemical reactivity under vibrational coupling to the vacuum electromagnetic field. *Angew. Chem., Int. Ed.* **2016**, *55*, 11634−11638.

(14) Thomas, A.; Lethuillier-Karl, L.; Nagarajan, K.; Vergauwe, R. M.; George, J.; Chervy, T.; Shalabney, A.; Devaux, E.; Genet, C.; Moran, J.; Ebbesen, T. W. Tilting a ground-state reactivity landscape by vibrational strong coupling. *Science* **2019**, *363*, 615−619.

(15) Ahn, W.; Herrera, F.; Simpkins, B. Modification of Urethane Addition Reaction via Vibrational Strong Coupling. April 05, *ChemRxiv* **2022**, DOI: DOI: 10.26434/chemrxiv-2022-wb6vs (accessed December 28, 2022).

(16) Vergauwe, R. M.; Thomas, A.; Nagarajan, K.; Shalabney, A.; George, J.; Chervy, T.; Seidel, M.; Devaux, E.; Torbeev, V.; Ebbesen, T. W. Modification of enzyme activity by vibrational strong coupling of water. *Angew. Chem., Int. Ed.* **2019**, *58*, 15324−15328.

(17) Lather, J.; George, J. Improving enzyme catalytic efficiency by co-operative vibrational strong coupling of water. *J. Phys. Chem. Lett.* **2020**, *12*, 379−384.

(18) Sau, A.; Nagarajan, K.; Patrahau, B.; Lethuillier-Karl, L.; Vergauwe, R. M.; Thomas, A.; Moran, J.; Genet, C.; Ebbesen, T. W. Modifying woodward−hoffmann stereoselectivity under vibrational strong coupling. *Angew. Chem., Int. Ed.* **2021**, *60*, 5712−5717.

(19) Hirai, K.; Takeda, R.; Hutchison, J. A.; Uji-i, H. Modulation of Prins cyclization by vibrational strong coupling. *Angew. Chem., Int. Ed.* **2020**, *59*, 5332−5335.

(20) Fukushima, T.; Yoshimitsu, S.; Murakoshi, K. Inherent Promotion of Ionic Conductivity via Collective Vibrational Strong Coupling of Water with the Vacuum Electromagnetic Field. *J. Am. Chem. Soc.* **2022**, *144*, 12177−12183.

(21) Chen, T. T.; Du, M.; Yang, Z.; Yuen-Zhou, J.; Xiong, W. Cavity-enabled enhancement of ultrafast intramolecular vibrational redistribution over pseudorotation. *Science* **2022**, *378*, 790−794.

(22) Li, T. E.; Nitzan, A.; Subotnik, J. E. Collective vibrational strong coupling effects on molecular vibrational relaxation and energy transfer: Numerical insights via cavity molecular dynamics simulations. *Angew. Chem., Int. Ed.* **2021**, *133*, 15661−15668.

(23) Du, M.; Yuen-Zhou, J. Catalysis by dark states in vibropolaritonic chemistry. *Phys. Rev. Lett.* **2022**, *128*, No. 096001.

(24) Li, T. E.; Nitzan, A.; Subotnik, J. E. Energy-efficient pathway for selectively exciting solute molecules to high vibrational states via solvent vibration-polariton pumping. *Nat. Commun.* **2022**, *13*, 1−8.

(25) Schäfer, C.; Flick, J.; Ronca, E.; Narang, P.; Rubio, A. Shining light on the microscopic resonant mechanism responsible for cavity-mediated chemical reactivity. *Nat. Commun.* **2022**, *13*, 1−9.

(26) Xiang, B.; Ribeiro, R. F.; Dunkelberger, A. D.; Wang, J.; Li, Y.; Simpkins, B. S.; Owrutsky, J. C.; Yuen-Zhou, J.; Xiong, W. Two-dimensional infrared spectroscopy of vibrational polaritons. *PNAS* **2018**, *115*, 4845−4850.

(27) Hirai, K.; Ishikawa, H.; Chervy, T.; Hutchison, J. A.; Uji-i, H. Selective crystallization via vibrational strong coupling. *Chem. Sci.* **2021**, *12*, 11986−11994.

(28) Sandeep, K.; Joseph, K.; Gautier, J.; Nagarajan, K.; Sujith, M.; Thomas, K. G.; Ebbesen, T. W. Manipulating the Self-Assembly of Phenyleneethynylenes under Vibrational Strong Coupling. *J. Phys. Chem. Lett.* **2022**, *13*, 1209−1214.

(29) Joseph, K.; Kushida, S.; Smarsly, E.; Ihiawakrim, D.; Thomas, A.; Paravicini-Bagliani, G. L.; Nagarajan, K.; Vergauwe, R.; Devaux, E.; Ersen, O.; Bunz, U. H.; Ebbesen, T. W. Supramolecular assembly of conjugated polymers under vibrational strong coupling. *Angew. Chem., Int. Ed.* **2021**, *60*, 19665−19670.

(30) Lather, J.; Bhatt, P.; Thomas, A.; Ebbesen, T. W.; George, J. Cavity catalysis by cooperative vibrational strong coupling of reactant and solvent molecules. *Angew. Chem., Int. Ed.* **2019**, *58*, 10745−10748.

(31) Lather, J.; Thabassum, A. N.; Singh, J.; George, J. Cavity catalysis: modifying linear free-energy relationship under cooperative vibrational strong coupling. *Chem. Sci.* **2021**, *13*, 195−202.

(32) Tavis, M.; Cummings, F. W. Exact solution for an N-molecule—Radiation-field Hamiltonian. *Phys. Rev.* **1968**, *170*, 379−384.

(33) Haugland, T. S.; Schäfer, C.; Ronca, E.; Rubio, A.; Koch, H. Intermolecular interactions in optical cavities: An ab initio QED study. *J. Chem. Phys.* **2021**, *154*, No. 094113.

(34) Flick, J.; Schäfer, C.; Ruggenthaler, M.; Appel, H.; Rubio, A. Ab initio optimized effective potentials for real molecules in optical cavities: Photon contributions to the molecular ground state. *ACS Photonics* **2018**, *5*, 992−1005.

(35) Pavošević, F.; Hammes-Schiffer, S.; Rubio, A.; Flick, J. Cavity-modulated proton transfer reactions. *J. Am. Chem. Soc.* **2022**, *144*, 4995−5002.

(36) Reichardt, C. Empirical parameters of solvent polarity as linear free-energy relationships. *Angew. Chem., Int. Ed.* **1979**, *18*, 98−110.

(37) Cerón-Carrasco, J. P.; Jacquemin, D.; Laurence, C.; Planchat, A.; Reichardt, C.; Sraïdi, K. Solvent polarity scales: determination of new ET(30) values for 84 organic solvents. *J. Phys. Org. Chem.* **2014**, *27*, 512−518.

(38) Plenert, A. C.; Mendez-Vega, E.; Sander, W. Micro-vs Macrosolvation in Reichardt's Dyes. *J. Am. Chem. Soc.* **2021**, *143*, 13156−13166.

(39) Reichardt, C. Solvatochromic Dyes as Solvent Polarity Indicators. *Chem. Rev.* **1994**, *94*, 2319−2358.

(40) Reichardt, C. Solvatochromism, thermochromism, piezochromism, halochromism, and chiro-solvatochromism of pyridinium N-phenoxide betaine dyes. *Chem. Soc. Rev.* **1992**, *21*, 147−153.

(41) Catalán, J.; de Paz, J. L. G.; Reichardt, C. On the Molecular Structure and UV/vis Spectroscopic Properties of the Solvatochromic and Thermochromic Pyridinium-N-Phenolate Betaine Dye B30. *J. Phys. Chem. A* **2010**, *114*, 6226−6234.

(42) Kumar, R. S.; Jeong, J.; Mergu, N.; Oh, W.; Son, Y. A. Solvent effect on the thermochromism of new betaine dyes. *Dyes Pigm.* **2017**, *136*, 458−466.

(43) Machado, C.; da Graça Nascimento, M.; Rezende, M. C.; Beezer, A. E. Calorimetric evidence of aggregation of the ET(30) dye in alcoholic solutions. *Thermochim. Acta* **1999**, *328*, 155−159.

(44) Pang, Y.; Thomas, A.; Nagarajan, K.; Vergauwe, R. W. A.; Joseph, K.; Patrahau, B.; Wang, K.; Genet, C.; Ebbesen, T. W. On the Role of Symmetry in Vibrational Strong Coupling: The Case of Charge-Transfer Complexation. *Angew. Chem., Int. Ed.* **2020**, *59*, 10436−10440.

(45) Halevi, E. A. Polarity differences between deuterated and normal molecules. *Trans. Faraday Soc.* **1958**, *54*, 1441−1446.

(46) Turowski, M.; Yamakawa, N.; Meller, J.; Kimata, K.; Ikegami, T.; Hosoya, K.; Tanaka, N.; Thornton, E. R. Deuterium isotope effects on hydrophobic interactions: the importance of dispersion interactions in the hydrophobic phase. *J. Am. Chem. Soc.* **2003**, *125*, 13836−13849.

https://doi.org/10.1021/jacs.3c02260
J. Am. Chem. Soc. XXXX, XXX, XXX−XXX

(47) Shi, C.; Zhang, X.; Yu, C. H.; Yao, Y. F.; Zhang, W. Geometric isotope effect of deuteration in a hydrogen-bonded host−guest crystal. *Nat. Commun.* **2018**, *9*, 1−9.
(48) Wade, D. Deuterium isotope effects on noncovalent interactions between molecules. *Chem.-Biol. Interact.* **1999**, *117*, 191−217.
(49) Van Hook, W. A.; Wolfsberg, M. Comments on H/D Isotope Effects on Polarizabilities of Small Molecules. Correlation with Virial Coefficient, Molar Volume, and Electronic Second Moment Isotope Effects. *Z. Naturforsch. A* **1994**, *49*, 563−577.
(50) Eisenschitz, R.; London, F. Über das Verhältnis der van der Waalsschen Kräfte zu den homöopolaren Bindungskräften. *Z. Phys.* **1930**, *60*, 491−527.
(51) Connolly, M. L. Solvent-accessible surfaces of proteins and nucleic acids. *Science* **1983**, *221*, 709−713.
(52) Connolly, M. L. Computation of molecular volume. *J. Am. Chem. Soc.* **1985**, *107*, 1118−1124.
(53) Philbin, J. P.; Haugland, T. S.; Ghosh, T. K.; Ronca, E.; Chen, M.; Narang, P.; Koch, H. Molecular van der Waals fluids in cavity quantum electrodynamics. September 16, **2022**, *arXiv*, arXiv:2209.07956, DOI: DOI: 10.48550/arXiv.2209.07956 (accessed December 29, 2022).
(54) Fowkes, F. M. Additivity of intermolecular forces at interfaces. i. determination of the contribution to surface and interfacial tensions of dispersion forces in various liquids. *J. Phys. Chem.* **1963**, *67*, 2538−2541.
(55) Nolte, C.; Ammer, J.; Mayr, H. Nucleofugality and nucleophilicity of fluoride in protic solvents. *J. Org. Chem.* **2021**, *77*, 3325−3335.

https://doi.org/10.1021/jacs.3c02260
J. Am. Chem. Soc. XXXX, XXX, XXX−XXX